Proceedings 10th NUMGE 2023
10th European Conference on Numerical Methods in Geotechnical Engineering
Zdravkovic L, Kontoe S, Taborda DMG, Tsiampousi A (eds)

https://doi.org/10.53243/NUMGE2023-396

A numerical investigation for computing effective elastic stiffness of bonded geomaterials

S. Srivastav[1], A.N. Roy Chowdhury[1], A. Das[1], V. Patel[2]

[1]*Department of Civil Engineering, Indian Institute of Technology Kanpur, India*
[2] *School of Computing, Engineering and Mathematical Sciences, La Trobe University, Bendigo, VIC, Australia*

ABSTRACT: Rocks and concretes are large particle-reinforced composites where a hardened cementitious matrix bonds the grains. Analytical or numerical homogenisation is often performed on a representative unit cell to estimate the effective elastic constants of such particle-reinforced composites. In this work, we have proposed a framework to analyse the effect of variation of gradation on the effective elastic modulus of large particle-reinforced composites. In this work, we aim to examine the accuracy of the various analytical homogenization schemes for estimating the elastic modulus of bonded geomaterial. Accuracies of the various analytical homogenization schemes are ascertained by comparing the analytical estimates with the results obtained from crushing tests simulated by finite element analysis. Multiple finite element analyses were performed on various representative volume elements with different particle volume fractions and arrangements. From the crushing tests, force deformation curves are obtained from which the effective elastic constants of the aggregates are estimated. The estimated effective elastic constants are then used for determining the upper-bound and lower-bound values of the effective elastic constants of the particle-reinforced composites. It is observed that homogenisation based on equal stress, i.e. the Reuss model, gives the best estimate of elastic constant for composite with uniformly graded particulate reinforcement.

Keywords: Cementitious composite, Inclusion, Finite Elements, Elastic stiffness, Aggregate gradation

1 INTRODUCTION

Geologic composites such as sandstone and calcarenite, as well as engineering materials like concrete and bitumen mixture, have a common mesoscale structure. Both types of composites consist of multiphase structures involving grains and bonding cement or porous matrix in general (Chen et al., 2022). The individual properties of different phases may vary depending on the mineralogy (Prasad et al., 2009, Khadem et al., 2021), which affects the macroscopic response of these composites, including stiffness, strength, and fracture pattern. Load transfer mechanisms through the grain and matrix also vary depending on the relative difference of individual phases.

These composites have numerous uses within civil engineering, from buildings to tunnels, nuclear reactors, and bridges. Predictive material models typically use an average material response of these composites. Microstructurally inspired models, on the other hand, require individual properties of different phases of the composite to capture the effects of material heterogeneity and anisotropy on the macroscopic response (Damien et al., 2019). However, these models also require an appropriate homogenization scheme for the continuum description of the material.

Since the early 1960s, there has been significant research on the elastic properties of heterogeneous materials, possibly due to the interest in creating composite engineering materials with specific characteristics. Most of this work is fundamental and offers a solid framework for comprehending and discussing the characteristics of aggregates and composite materials (Contrafatto et al., 2016; Raju et al., 2018).

Mixture theory-based parallel (Voigt, 1889) and series (Reuss, 1929) models based on mixture theory provide the limits of elastic stiffness for two-phase composites. However, modelling complex composites like rocks and concrete requires additional understanding based on micromechanics and an appropriate homogenization scheme to determine effective elastic properties. The Mori-Tanaka model based on Eshelby's equivalent inclusion theory (Mori and Tanaka, 1973) is one of the most popular models for composites. The Mori-Tanaka approach, however, has a major limitation in that the microstructure is assumed to be homogeneous, ignoring the effects of inclusion size and number (Gong et al., 2011).

In recent years, several advanced homogenization schemes have been developed to address the inherent limitations of the Mori-Tanaka model (Saadt et al., 2015; Contrafatto et al., 2016; Damien et al., 2019). However, most of these analytical models do not

consider the effects of variation in inclusion size and gradation.

The objective of this study is to randomly build representative volume element (RVE) of composite having distinct granular structure and matrix using a given set of parameters and a random distribution of the coordinates and sizes of the solid inclusions. To examine how the mesostructure constituents influence the macroscopic elastic response of the composite material, the resulting models are meshed using an automatic meshing pre-processor prior to computational testing with the finite element (FE) code ABAQUS. Finally, the results (elastic stiffness) are compared with various analytical models.

2 METHODS OF ANALYSIS

2.1 Particle packing RVE generation

This study focuses on analysing composite stiffness by considering typical microstructural properties of concrete. Concrete is chosen because it has a lower level of heterogeneity compared to geologic composites. Additionally, the granular structure (aggregate) and the matrix (mortar) have significantly different elastic properties, allowing for easy identification of the individual phases' influence. Here pores are assumed to be part of the matrix in this study.

Aggregates typically account for 50–70 percent of the concrete volume and significantly impact its characteristics, mix proportions, and economics. Sand, gravel, and crushed stone are the most commonly utilised aggregates. Fine and coarse aggregates are the two main types, with fine aggregates typically passing through a sieve with a 4.75-mm opening, while coarse aggregates are any particles with a diameter greater than 4.75 mm.

Most of the coarse aggregate utilized in concrete consists of gravel, while crushed stone comprises the majority of the remaining portion. The shape of the aggregate particles is dependent on the type of aggregate.

The composite behaviour of concrete is influenced by the random scattering of aggregate particles, with the spaces between them filled by the mortar matrix. The arrangement of the matrix is determined solely by the distribution of aggregate particles, meaning it is unnecessary to evaluate it separately. Instead, an RVE (Representative Volume Element) was generated to analyse the composite behaviour. For simplicity, the particles were assumed to be spherical in shape. Three different grading curves, as shown in Fig. 1, were used to generate the particles. It should be noted that the grading curves were selected such that the particle diameter corresponding to 50% fineness was the same in all cases.

For each grading, four cubic RVEs are created, each with coarse aggregate volume fractions of 60%, 50%, 40%, and 20%. The size of RVEs is within a range of 40 mm to 49 mm depending on the convergence in packing generation, avoiding any overlap among the particles while maintaining the appropriate volume fraction. A typical packing for grading 2 with a 60% volume fraction is depicted in Fig 2. The granular packing is generated using the discrete element code PFC3D.

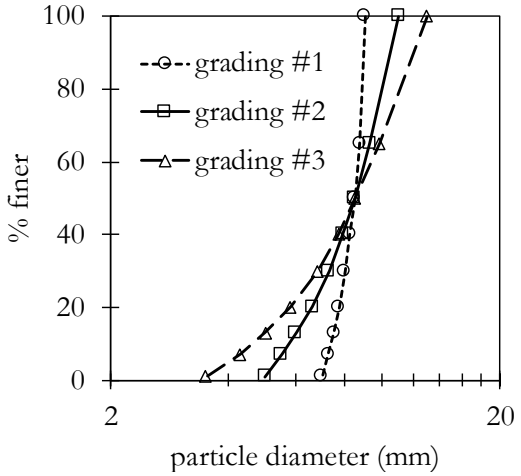

Figure 1. Coarse aggregate grading curves

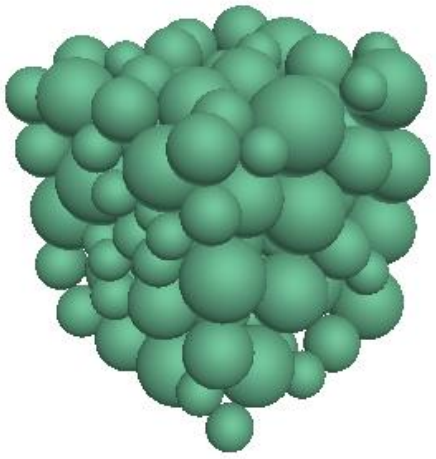

Figure 2. Typical packing of coarse aggregate (60% volume fraction for grading #2)

2.2 Finite element model

In this work, we aim to examine the accuracy of the various analytical homogenization schemes for estimating the elastic modulus of bonded geomaterial. Accuracies of the various analytical homogenization schemes are ascertained by comparing the analytical estimates with the results obtained from crushing tests simulated by finite element analysis. Multiple finite element analyses were performed on various representative volume elements with different particle volume fractions and arrangements. The granular packing generated previously is imported into the 3D finite element code ABAQUS and placed in a cubic domain, with the voids filled with mortar. The elasticity constants for the different phases are 62 GPa and 19 GPa for aggregate and mortar, respectively, with Poisson's ratio considered 0.2 for both phases which are obtained from Wriggers and Moftah

(2006). The domain is meshed with eight-node tetrahedral elements (C3D8). Appropriate displacement boundary conditions are provided to avoid any rigid body translation or rotation during compression. Crushing tests are simulated by subjecting the RVE to a displacement-controlled uniaxial compression where the lateral surfaces of the RVE are kept unconfined. In the analysis, the bottom boundary is restrained from vertical movement, while the top boundary is subjected to displacement control compression. A typical cross-section of the FE model is shown in Fig. 3, with the dark (green online) circular segments indicating the inclusions and the remaining white portion referring to the matrix.

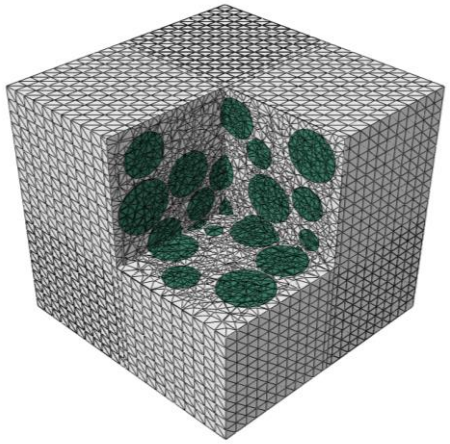

Figure 3. Typical cross-sectional view and meshing of a FE model

2.3 Analytical Models

In the present study, five different mixture theory-based models, namely Voigt, Reuss, H-S, Chamis, and H-T models, are assessed to determine the effective composite stiffness. The basic formulation of each model is briefly presented here. The common notations are the following: E, K and G refer to Young's modulus, bulk modulus and shear modulus, respectively; V is the volume fraction of a given phase; the subscripts, eff, m, f, L, and U refer to the effective, matrix, inclusion, lower bound and upper bound properties, respectively.

Voigt (1889) model considers equal strain in both the matrix and the fiber inclusion of the composite. The effective elastic Young's modulus of composite in a one-dimensional scenario is given by,

$$E_{eff} = E_f V_f + E_m(1 - V_f) \tag{1}$$

Reuss (1929) model assumes equal stress in different phases of the composite. The effective elastic modulus is given by,

$$\frac{1}{E_{eff}} = \frac{V_f}{E_f} + \frac{(1-V_f)}{E_m} \tag{2}$$

H-S or Hashin-Shtrikmanare (1963) proposed the upper and lower bounds of composite stiffness from strain energy calculation. A polarization stress tensor is utilized to obtain the maximum and minimum bounds in strain energy. The effective modulus in H-S model based on bulk (K) and shear (G) moduli are given by,

$$K_{eff}\big|_L = K_m + \frac{V_f}{\left[(K_f - K_m)^{-1} + V_m\left(K_m + \frac{4}{3}G_m\right)^{-1}\right]} \tag{3a}$$

$$K_{eff}\big|_U = K_f + \frac{V_m}{\left[(K_m - K_f)^{-1} + V_f\left(K_f + \frac{4}{3}G_f\right)^{-1}\right]} \tag{3b}$$

$$G_{eff}\big|_L = G_m + \frac{V_f}{\left[(G_f - G_m)^{-1} + \frac{6V_m(K_m+2G_m)}{5G_m(3K_m+4G_m)}\right]} \tag{3c}$$

$$G_{eff}\big|_U = G_f + \frac{V_m}{\left[(G_m - G_f)^{-1} + \frac{6V_f(K_f+2G_f)}{5G_f(3K_f+4G_f)}\right]} \tag{3d}$$

Chamis (1984) proposed effective transverse elastic moduli (E_{22}) of the composite based on inclusion packing geometry. Eq. 4 shows a simplified version of the same.

$$E_{22} = \frac{E_m}{1 - \sqrt{V_f}\left(1 - \frac{E_m}{E_{22f}}\right)} \tag{4}$$

Halpin and Tsai (Halpin, 1969) model or the H-T model, is an empirical fitting model that improves over other models using an appropriate fitting parameter (ξ) which estimates $\xi = 1 + 40V_f$. In this model, the effective Young's modulus is given by

$$\frac{E_{eff}}{E_m} = \frac{1+\xi\eta V_f}{1-\eta V_f}, \eta = \left[\frac{E_f}{E_m} - 1\right]\left[\frac{E_f}{E_m} + \xi\right]^{-1} \tag{5}$$

A comprehensive review of the performance of individual models can be found in Raju et al. (2018). It is crucial to notice that all these models are primarily effective for composites with an organized pattern of inclusions. In order to examine the heterogeneity of inclusions, like aggregates in concrete, the homogenization-based Mori-Tanaka model (Benveniste, 1987) is also considered. The detailed formulation of the Mori-Tanaka model is not presented here to avoid repetition, but it can be found in Gross and Seelig (2011).

3 RESULTS & DISCUSSION

3.1 Finite element analysis

The vertical stress-strain response, given in Fig. 4 (few typical), obtained from FE analysis shows a linear trend

for all aggregate volume fraction combinations and gradation combinations. Such a response is expected since linear elasticity is considered in both phases of the cementitious composite.

The analysis further indicates that stiffness (Young's modulus) linearly increases with increasing aggregate volume fraction. Fig. 5 shows the evolution of stiffness for all the FE simulations. However, stiffness appears to be reducing with wider gradation compared to uniform gradation (grading #1).

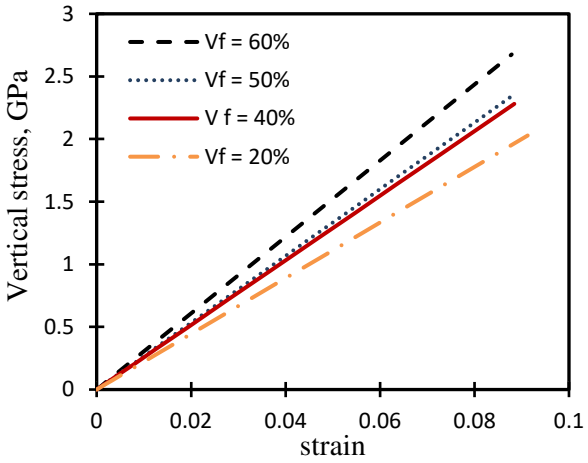

Figure 4. Typical stress-strain response for FE model with grading #2

The mean particle size (d_{50}) is identical in all three gradations. Therefore, in the case of a wider distribution (e.g., gradation #3), the total inclusion surface area is smaller than the sample with uniform gradation, even for the same volume fraction. Thus, in different sections of the composite, load transfer only occurs through the matrix and consequently reduces stiffness. Such a phenomenon is pronounced for specimens with a higher volume fraction of inclusion.

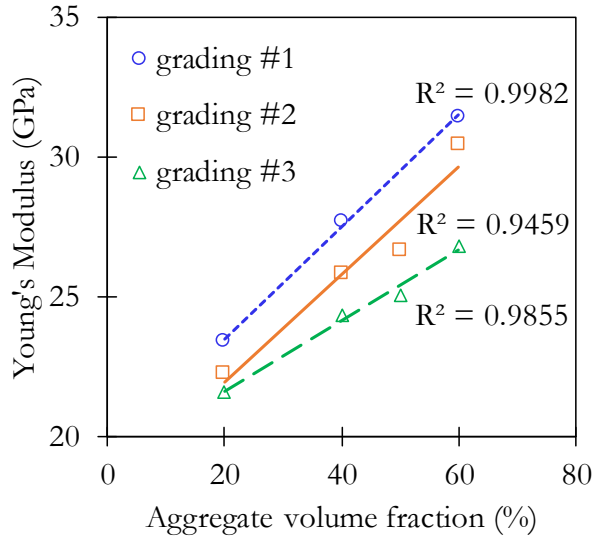

Figure 5. Computed elastic modulus with variation in aggregate grading and volume fraction.

Vertical stress and strain contours are plotted in Fig. 6 for a typical composite (grading #1, V_f= 50%). The stress field demonstrates a mixed variation within the inclusions and matrix. In some cases, the boundaries between the phases are not distinguishable, indicating the same stress field. On the other hand, the vertical strain field across the inclusions is distinct compared to the matrix. The upper and lower limits of the strain field show a larger variation (10 times) than the stress field (5 times).

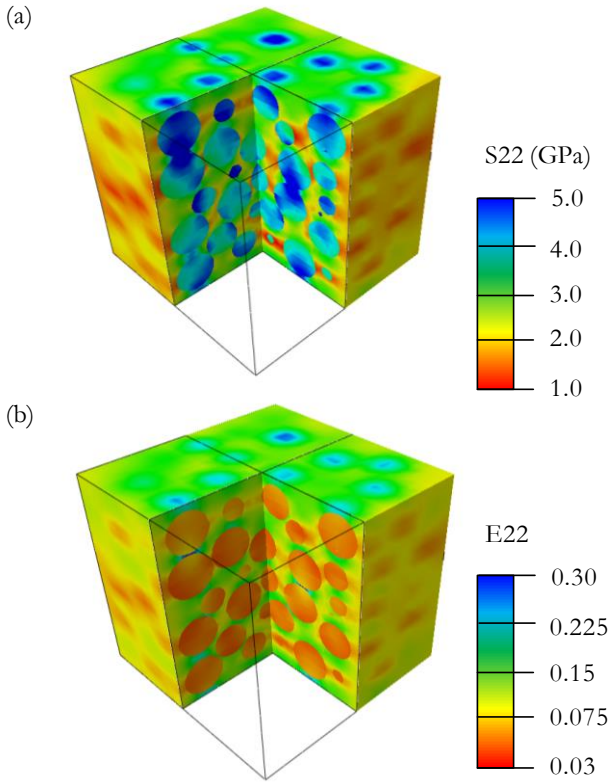

Figure 6. Vertical stress (a, S_{22}) *and strain* (b, E_{22}) *contour in a FE model*

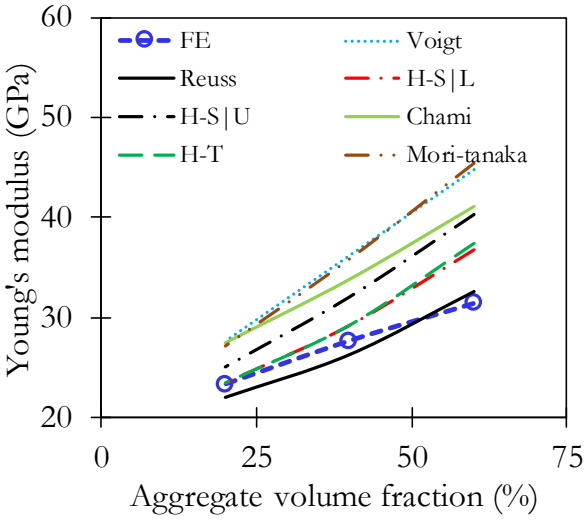

Figure 7. Comparison among the analytical models.

3.2 *Analytical Model response*

All the discussed analytical models are used to determine the effective Young's modulus of the composite. For analytical models, stiffness and volume

fraction of individual phases (mortar and aggregate) are used. However, none of the models captures the gradation variation. Hence it is assumed that the analytical models can only predict the composite with uniform gradation. In the present study, grading #1 represents particle size close to a uniform gradation.

Figure 7 compares different model responses along with FE analysis for grading #1. The results indicate Reuss model agrees well with the FE analysis. This observation corroborates the spatial distribution of stress and strain across the composite shown in Fig. 6. Unlike the strain field, the stress field does not show a distinct variation between the inclusion and matrix. Similarly, in the Reuss model, the main argument is equal stress across different phases of a composite.

4 CONCLUSIONS

In the present study, we show the effect of inclusion size in terms of gradation on the elastic response of cemented composites. Finite element models are prepared to compute the elastic stiffness. The results show that models with uniformly graded inclusion are stiffer than those with well-graded inclusion despite having identical mean particle sizes and volume fractions. Such elastic stiffness alteration likely happens due to the variation in inclusion surface area in different gradations. Further, different analytical models are employed to capture the composite elastic stiffness parameters. The equal stress-based Reuss model agrees well against the uniformly graded inclusion specimen. However, none of the analytical models was suitable for capturing gradation effects. It appears additional scaling should be imposed to account for the gradation variation while computing elastic stiffness in composites. This work is in preparation and will be presented in future publications.

5 REFERENCES

Benveniste, Y. 1987. New approach to the application of Mori-Tanaka's theory, 6, 147–57

Chamis, C.C., 1984, October. Mechanics of composite materials: past, present and future, In 21st annual meeting of the society for engineering science (No. E-3936) 11, 3–14

Chen, B., Xiang, J., Latham, J. 2023. Influence of inter-grain cementation stiffness on the effective elastic properties of porous Bentheim sandstone. Journal of Rock Mechanics and Geotechnical Engineering. 15 (3), 573-583, 10.1016/J.JRMGE.2022.06.009

Contrafatto, L., Cuomo, M., Gazzo, S. 2016. A concrete homogenisation technique at meso-scale level accounting for damaging behaviour of cement paste and aggregates, Computers & Structures 173, 1-18. https://doi.org/10.1016/j.compstruc.2016.05.009

Damien, D., Wang, Y., Xi, Y. 2019. Prediction of elastic properties of cementitious materials based on multiphase and multiscale micromechanics theory, Journal of Engineering Mechanics 145(10), 04019074.

Gong, S., Li, Z., Zhao, Y. 2011. An extended Mori–Tanaka model for the elastic moduli of porous materials of finite size, Acta Materialia 59(17), 6820–6830.

Gross, D., Seelig, T. 2017. Fracture mechanics: with an introduction to micromechanics. Springer.

Halpin, J.C., 1969. Effects of environmental factors on composite materials. Technical report: Air Force Materials Lab Wright-Patterson AFB OH.

Hashin, Z., Shtrikman S.A. 1963. Variational approach to the theory of the elastic behaviour of multiphase materials, J Mech Phys Solids 11, 127–140

Khadem, B., Saberi, M.R., Avseth, P. 2021. Rock physics of sand-shale mixtures: Classifications, theoretical formulations and study on real dataset. Marine and Petroleum Geology 134, 105366. https://doi.org/10.1016/j.marpetgeo.2021.105366

Mori, T., Tanaka, K. 1973. Average stress in matrix and average elastic energy of materials with misfitting inclusions, Acta Metallurgica 21(5), 571-574. https://doi.org/10.1016/0001-6160(73)90064-3

Prasad, M., Pal-Bathija, A., Johnston, M., Rydzy, M., Batzle, M., 2009. Rock physics of the unconventional, Geophysics, The Leading Edge of Exploration 28(1), 34–38.

Raju, B., Hiremath, S., Roy Mahapatra, D. 2018. A review of micromechanics based models for effective elastic properties of reinforced polymer matrix composites, Composite Structures 204, 607-619. https://doi.org/10.1016/j.compstruct.2018.07.125

Reuss, A. 1929. Berechnung der fließgrenze von mischkristallen auf grund der plastizitätsbedingung für einkristalle, ZAMM-Journal of Applied Mathematics and Mechanics/Zeitschrift für Angewandte Mathematik und Mechanik 9(1), 49-58.

Saadat, F., Birman, V., Thomopoulos, S., Genin, G. M. 2015. Effective elastic properties of a composite containing multiple types of anisotropic ellipsoidal inclusions, with application to the attachment of tendon to bone, Journal of the Mechanics and Physics of Solids 82, 367-377. https://doi.org/10.1016/j.jmps.2015.05.017

Voigt, W. 1889. On the relationship between the two constants of elasticity of isotropic bodies, Annalen der physik, 274(12), 573-587.

Wriggers, P., Moftah, S. O., 2006. Mesoscale models for concrete: Homogenisation and damage behaviour, 42(7), 623-636.